Dopant-free star-shaped hole-transport materials for efficient and stable perovskite solar cells

11 authors, including:

Fei Zhang
Tianjin University
25 PUBLICATIONS   85 CITATIONS

SEE PROFILE

Shirong Wang
Tianjin University
59 PUBLICATIONS   512 CITATIONS

SEE PROFILE

Xianggao Li
58 PUBLICATIONS   505 CITATIONS

SEE PROFILE

Michael Graetzel
École Polytechnique Fédérale de Lausanne
927 PUBLICATIONS   98,222 CITATIONS

SEE PROFILE

Some of the authors of this publication are also working on these related projects:

Project   Cutting Edge Third Generation Advanced Photovoltaic Devices View project

Project   Perovskite solar cell View project

Dopant-free star-shaped hole-transport materials for efficient and stable perovskite solar cells

Fei Zhang [a, b, c], Xiaoming Zhao [a, c], Chenyi Yi [b], Dongqin Bi [b], Xiangdong Bi [d], Peng Wei [e], Xicheng Liu [a, c], Shirong Wang [a, c, *], Xianggao Li [a, c], Shaik Mohammed Zakeeruddin [b, f, **], Michael Grätzel [b, ***]

[a] School of Chemical Engineering and Technology, Tianjin University, 300072 Tianjin, China
[b] Laboratory of Photonics and Interfaces, Institute of Chemical Sciences and Engineering, École Polytechnique Fédérale de Lausanne (EPFL), Station 6, CH-1015 Lausanne, Switzerland
[c] Collaborative Innovation Center of Chemical Science and Engineering (Tianjin), 300072 Tianjin, China
[d] Department of Physical Sciences, Charleston Southern University, 9200 University Blvd., Charleston, SC 29485, USA
[e] Affinity Research Chemicals, Inc. 9 Germay Drive, Suite 300B, Wilmington, DE 19804, USA
[f] Center of Excellence for Advanced Materials Research (CEAMR), King Abdulaziz University, Jeddah, Saudi Arabia

ARTICLE INFO

ABSTRACT

Two star-shaped TPA-based small-molecule materials (Z1012 and Z1013) were designed and synthesized in this paper. These molecules show high hole mobility and suitable energy levels for $CH_3NH_3PbI_3$-based perovskite solar cells. Photovoltaic cells based on the Z1013 without any dopants or additives achieve an excellent power conversion efficiency (PCE) of 15.4%, which is comparable to devices based on state-of-art p-doped *spiro*-OMeTAD. Moreover, the devices based on these two HTMs show much better stability than that of devices based on *spiro*-OMeTAD when aging in ambient air both at room temperature and 80 °C. These results demonstrate that star-shape TPAs could be excellent dopant-free HTMs for perovskite solar cells and hold promise to replace the p-doped *spiro*-OMeTAD, which is important for the fabrication of cost-effective and stable devices.

© 2016 Published by Elsevier Ltd.

1. Introduction

Organic—inorganic hybrid perovskite solar cells (e.g. (RNH_3) PbX_3 (R = alkyl, X = halogen)) have been recently receiving great attention owing to their outstanding features such as superb photovoltaic performance and low cost [1–4]. Since hybrid perovskite solar cells were first demonstrated by Kojima et al., cells based on such materials have shown an unprecedented increase of power conversion efficiency (PCE) to 22.1% in subsequent years [5–7].

The best performing device configuration of perovskite solar cell (PSC) is based on mesoporous TiO_2 scaffold, which is infiltrated with perovskite material and coated with the hole-transport materials (HTMs) [8]. Electrons and holes were produced in the perovskite absorber upon photo-excitation, the electrons were diffused to the TiO_2, and the holes were transferred to the HTMs. These photo-generated charge carriers are subsequently collected as photocurrent at the front and back contacts of the solar cell [2,9]. To date, a great number of HTMs have been developed and incorporated in PSCs, which are composed of organic and inorganic hole-conductors [9]. Among the organic semiconductors, triphenyl-amine (TPA) containing compounds 2,2′,7,7′-tetrakis (N,N′-di-*p*-methoxy-phenylamine)-9,9′-spirobifluorene (*spiro*-OMeTAD) along with poly-triarylamine (PTAA) have shown to be most effective. However, their relatively high cost of synthesis along with the need to use high levels of dopants present caveats for practical applications. The dopants and additives in the HTMs contribute to
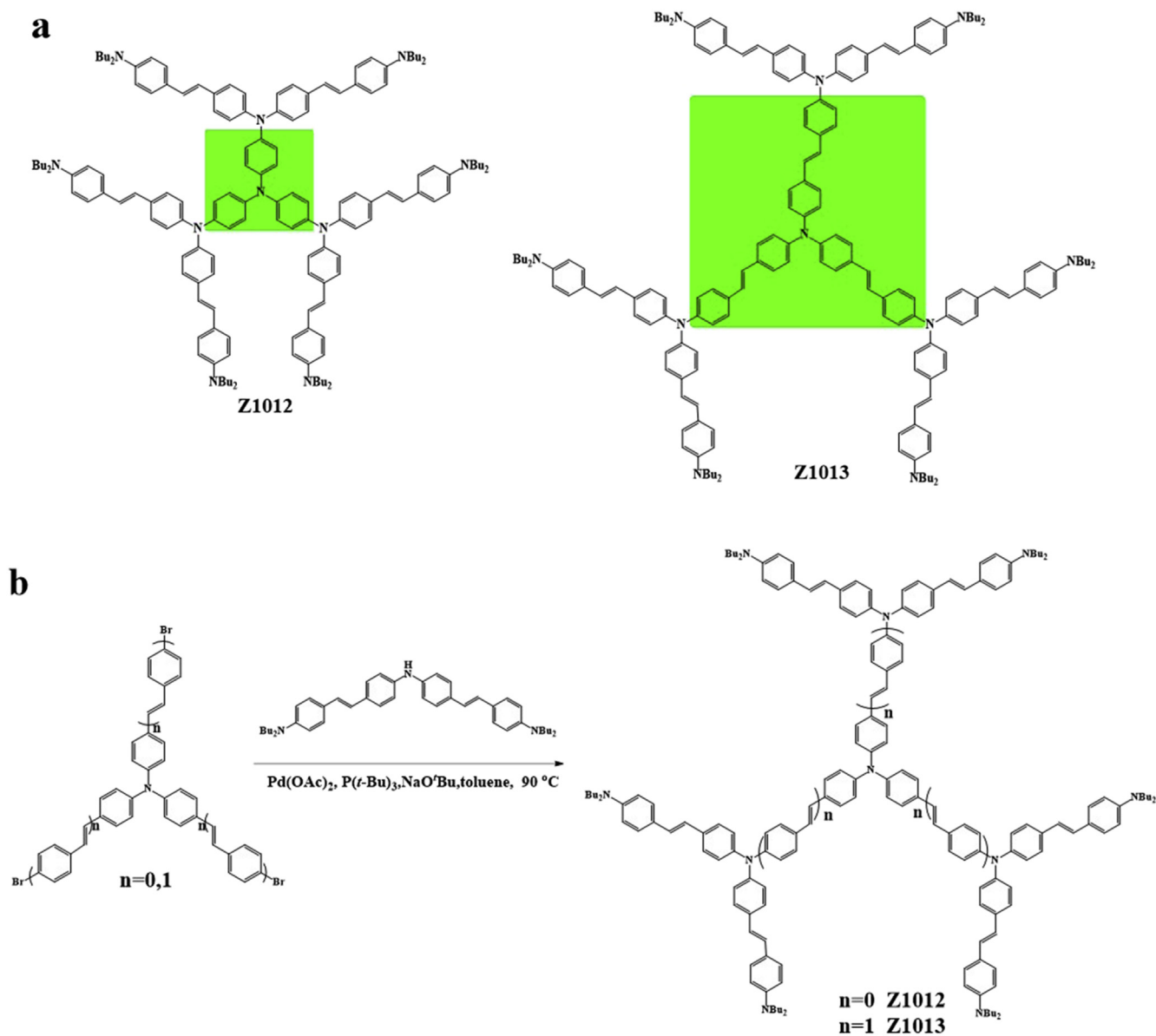
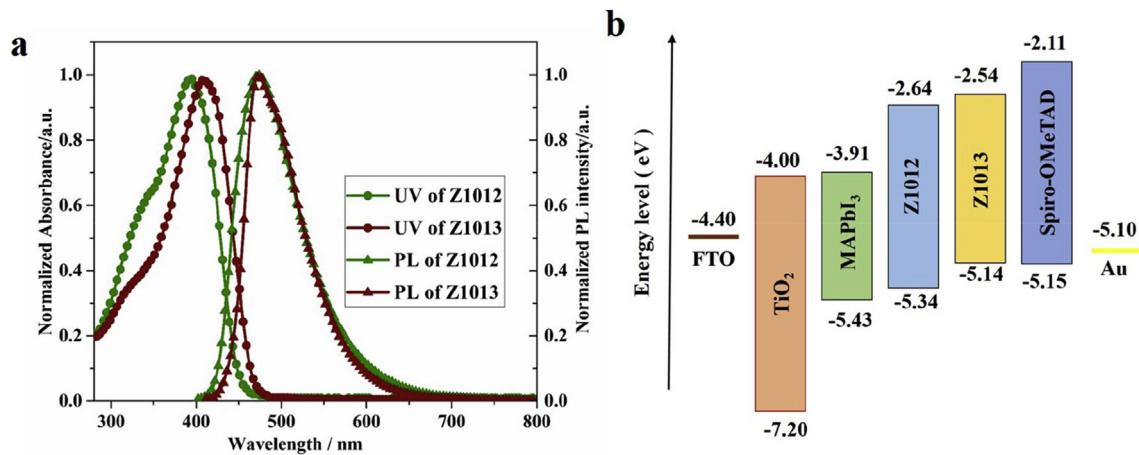**Fig. 1.** (a) Molecular structures of Z1012 and Z1013; (b) Synthetic route for Z1012 and Z1013.

Fig. 2. (a) UV—Vis absorption and photoluminescence spectra of Z1012 and Z1013 in THF solution (c = 1.0 × 10^{-5} mol L^{-1}); (b) Energy level diagram of the corresponding materials used in perovskite solar cells.

Table 1
Photophysical, electrochemical data and thermal characteristics of Z1012 and Z1013.

	abs (nm)	E_g (eV)	HOMO (eV)	LUMO (eV)	T_g (°C)
Z1012	393	2.70[a]	−5.34[a]	−2.64[a]	154.2
		2.96[b]	−4.58[b]	−1.62[b]	
Z1013	408	2.60[a]	−5.14[a]	−2.54[a]	171.8
		2.87[b]	−4.47[b]	−1.60[b]	

[a] Experimental values (HOMO levels are measured by cyclic voltammetry).
[b] Theoretical calculation values; $E_{LUMO} = E_{HOMO} + E_g$.

Table 2
Hole mobilities and reorganization energies of Z1012, Z1013 and *spiro*-OMeTAD.

HTM	Hole mobility ($cm^2 V^{-1} s^{-1}$)[a]	λ_1 (eV)[b]	λ_2 (eV)[c]	λ (eV)[d]
Z1012	9.74×10^{-5}	0.067	0.075	0.142
Z1013	6.67×10^{-4}	0.036	0.032	0.068
spiro-OMeTAD	2×10^{-4}	0.067	0.071	0.138

[a] Measured by Time-of-flight (TOF) method, details in ESI.
[b] $\lambda_1 = (E+^*)-(E+)$: Relaxation energy computed from the cation potential energy surface. $E+^*$ is the energy of the monomer cation at the neutral geometry, and E^* is the energy of the neutral monomer at the cation geometry.
[c] $\lambda_2 = (E^*)-E$: Relaxation energy computed from the neutral potential energy surface. $E+$ and E are the optimized energies of the cationic and neutral forms of a single monomer.
[d] λ (reorganization energy) $= \lambda_1 + \lambda_2$.

the low stability of the perovskite devices. Attempts have been made to develop more cost-effective and dopant-free HTMs for viable commercial applications of perovskite solar cell [10−23].

Star-shaped molecules feature a central core and multiple conjugated arms as functional units. They combine the advantages of both small molecules, i.e. well-defined structures and physical properties, and polymers like i.e. good thermal stabilities. They attracted much attention in organic solar cells as hole transporting materials in recent years [24−27]. Several star-shaped small molecule HTMs have been applied to PSCs [8,28−34]. However, these star-shaped HTMs exhibit relatively low PCEs and need dopants and additives.

Herein, two dopant-free TPA-based star-shaped HTMs (Z1012

and Z1013) were applied in PSCs. A PCE of 15.4% was achieved by Z1013 without doping under AM 1.5G (100 mW cm^{-2}) illumination, which matches to the PCE of p-doped *spiro*-OMeTAD (16.7%). This is among the highest efficiencies of the PSCs based on star-shaped HTMs. Importantly, these HTMs based devices shows a remarkable stability when aged in ambient air both at room tempreture and 80 °C in the dark.

2. Results and discussion

The chemical structures of the two HTMs are shown in Fig. 1a and the synthetic route for the two HTMs is depicted in Fig. 1b in line with our previous report [35]. Z1012 and Z1013 were synthesized through palladium-catalyzed amination of the branch molecule (E,E)-bis(4-(2-(4-N,N-dibutylaminophenyl)ethenyl)phenyl) amine with tris-(4-bromophenyl)amine and tris(4-((E)-4-bromostyryl)phenyl)amine, respectively. These two HTMs are having either triphenylamine or triphenylamine extending outward connected by phenylenevinylene units as the π-center. The triphenylamine displays good coplanarity of the central nitrogen and the three surrounding carbon atoms connecting to it, the triphenylamine unit can maintain uninterrupted conjugation between central nitrogen lone pair electrons and the arms, as well as function as a strong electron donor to the conjugation system [36,37]. The peripherally substituted amino groups further modulate the solubility of the molecule and provide more electron density to the structure. Both of them show good solubility in common organic solvents, such as dichloromethane, chloroform, tetrahydrofuran and toluene, etc.

We present the normalized UV−Vis absorption and photoluminescence (PL) spectra of Z1012 and Z1013 in THF solution in Fig. 2a and summarize relevant data in Table 1. The UV−vis absorption maximum due to a π-π* transition occurred at 393, and 408 nm, respectively, for molecule Z1012 and Z1013. This red shift in peak absorbance wavelength of Z1013 can be explained by a longer conjugation length, reducing the energy gap between HOMO and LUMO [35]. In addition, the PL spectra of the two HTMs show maximum emission at 473 and 474 nm respectively.

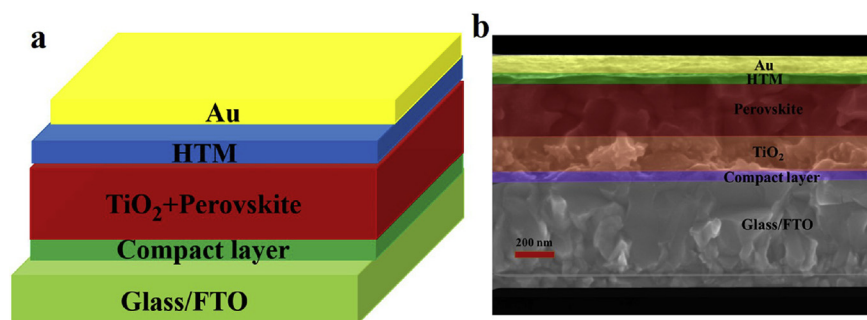Density functional theory (DFT) method with the Gaussian 03

Fig. 3. (a) Diagram of photovoltaic device structure; (b) Cross-sectional SEM image of the device based on Z1013 (at the concentration of 25 mg/mL).

Table 3
J-V curves of Z1012, Z1013 and *spiro*-OMeTAD based device under different scan directions with bias step of 5 mV.

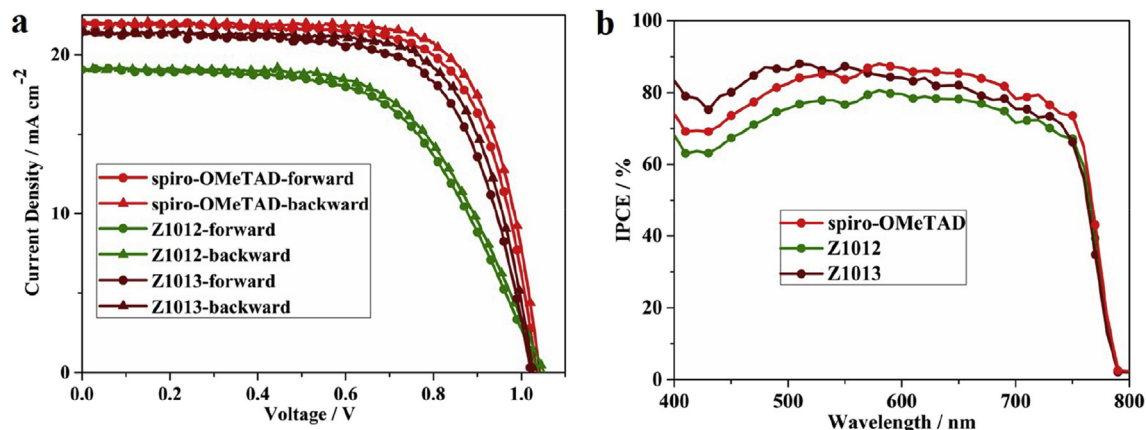| HTM	J_{sc} (mA cm^{-2})	V_{oc} (V)	FF	PCE (%)	Hysteresis index
spiro-OMeTAD (backward)	21.92	1.042	0.728	16.7	0.035
spiro-OMeTAD (forward)	22.05	1.035	0.701	16.1	
Z1012 (backward)	19.14	1.052	0.599	12.4	0.038
Z1012 (forward)	19.08	1.041	0.588	12.1	
Z1013 (backward)	21.33	1.027	0.702	15.4	0.034
Z1013 (forward)	21.45	1.022	0.671	14.7	

Fig. 4. (a) Current-voltage hysteresis curves of perovskite solar cells comprising champion devices with dopant-free Z1012, Z1013 and doped *spiro*-OMeTAD measured starting with backward scan and continuing with forward scan; (b) IPCE spectra of the devices based on Z1012, Z1013 without dopants and *spiro*-OMeTAD with additives and dopants.
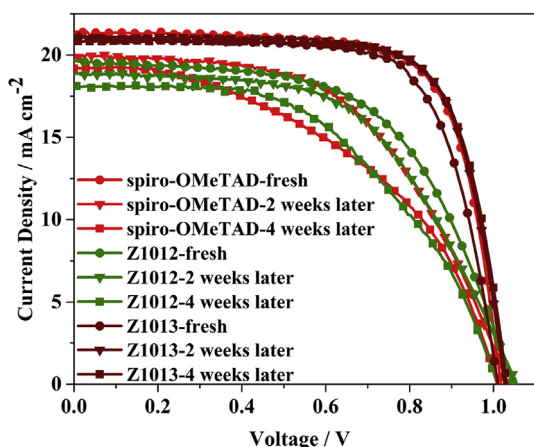

Fig. 5. Initial stability test of perovskite solar cells devices with dopant-free Z1012, Z1013 and doped *spiro*-OMeTAD at room temperature stored for 4 weeks.

program at the B3LYP/6-31G* level was used to predict the electronic properties of the Z1012 and Z1013. The optimized molecular geometries, the highest occupied molecular orbital (HOMO) and the lowest unoccupied molecular orbital (LUMO) are shown in Table S1. The LUMO is located mainly over the part of the peripheral units close to the triphenylamine core with some extending to the triphenylamine core. The HOMO spread mainly on the centered triphenylamine core and some extending to the adjacent aromatic rings of the peripheral units. The energy levels were also determined experimentally by cyclic voltammetry (CV). The CV result (Fig. S1a) shows that the HOMO energy level of Z1012 is at −5.34 eV, slightly lower than that of *spiro*-OMeTAD (−5.15 eV) [38]. Whereas the HOMO energy level of Z1013 is at −5.14 eV, similar to that of *spiro*-OMeTAD, as shown in Fig. 2b. Both match well the energy level of $CH_3NH_3PbI_3$ (−5.43 eV) [39].

The glass transition temperature (T_g) of Z1012 and Z1013 showed by differential scanning calorimetry (DSC) measurements is around 154.2 °C and 171.8 °C, respectively, which are substantially higher than that of *spiro*-MeOTAD ($T_g = 125$ °C), suggesting good morphology stability of Z1012 and Z1013 (Fig. S1b). We determined the hole transporting properties of Z1012 and Z1013 by performing time-of-flight (TOF) measurements (Fig. S2a,b). The hole mobilities of Z1012 and Z1013 are 9.74×10^{-5} cm^2 V^{-1} s^{-1} and 6.67×10^{-4} cm^2 V^{-1} s^{-1} at an electric field of 2.0×10^5 V cm^{-1},

respectively. The hole mobility of Z1013 is about 3.3 times higher than that of pristine *spiro*-OMeTAD (2×10^{-4} cm^2 V^{-1} s^{-1} at an electric field of 2.6×10^5 V cm^{-1}) [40]. The reorganization energy represents the relaxation of the molecule after oxidation or reduction, typically modeled by withdrawing or adding one electron. As indicated in Table 2, Z1013 has the lowest calculated reorganization energy, which agrees with the result of TOF test. This accelerates hole-transport over the other two HTMs [41].

A schematic diagram of the perovskite solar cell architecture applied in this study is shown in Fig. 3a. To confirm the device architecture, cross sectional scanning electron microscopy (SEM) measurements were carried out (Fig. 3b). Mesoporous titania can be clearly observed, with $CH_3NH_3PbI_3$ perovskite infiltrated and forming large crystals on top of the mesoporous photoanode.

The current-voltage (J−V) curves under standard AM 1.5G irradiation of 100 mW cm^{-2} is presented in Fig. 4a, S3a and photovoltaic performance metrics are summarized in Table 3, S2. The best cell of Z1013 affords an open-circuit voltage (V_{oc}) of 1.027 V, a short-circuit current density (Jsc) of 21.33 mA cm^{-2} and a fill factor (FF) of 0.702, yielding a PCE of 15.4% under AM 1.5G (100 mW cm^{-2}) illumination. This result is comparable to the PCE of 16.7% of *spiro*-OMeTAD doped with lithium bis(trifluoromethylsulfonyl)imide (LiTFSI) and 4-*tert*-butylpyridine (TBP). The devices based on Z1012 give a higher V_{oc} than that of *spiro*-OMeTAD, which is commensurate with its deeper HOMO level. However, devices based on Z1012 exhibit lower photovoltaic performance compared to Z1013 and *spiro*-OMeTAD, especially in terms of FF and J_{sc}, due to the lower hole mobility that impairs charge transfer in solar cells [9]. However, devices based on doped Z1012 and Z1013 exhibit lower photovoltaic performance compared to dopant-free Z1012 and Z1013. Apparently that means the dopants that work well with *spiro*-OMeTAD might not be suitable for these two HTMs [14]. Moreover, The dopants might have negative impact on the HTM film coverage which also can be seen from the SEM image (Fig. S4). We fabricated a batch of 10 cells each with Z1012, Z1013 and *spiro*-OMeTAD to examine the reproducibility of the cells' performance. The data is tabulated in Fig. S2c, indicating good device reproducibility. In our study a small hysteresis was also observed in the J−V curves and the hysteresis index calculated according to the equation [42] are 0.038, 0.034 and 0.035 for Z1012, Z1013 and *spiro*-OMeTAD based devices respectively. The stabilized power output were observed from devices based on *spiro*-OMeTAD, Z1012 and Z1013 is 16.4%,12.3% and 15.1% respectively (Fig. S5), which is consistent with the obtained PCE.

The incident photon-to-electron conversion efficiency (IPCE)

spectrum of the cells based on these three HTMs were shown in Fig. 4b. The integrated current densities estimated from the IPCE spectra is 19.09 mA cm^{-2} for Z1012, 20.56 mA cm^{-2} for Z1013 and $spiro$-OMeTAD, respectively, which are in excellent agreement with the J$_{sc}$ values obtained from the J-V curves.

We also compared the stability of Z1012, Z1013 and $spiro$-OMeTAD -based perovskite solar cells by exposing them continuously at room temperature and 80 °C in ambient air of 30% relative humidity in the dark without encapsulation. The current—voltage curves of typical cells were plotted in Fig. 5, S3b and the data were summarized in Table S3 and S4. The devices based-on Z1013 shows a slight increase of the PCE, while that based-on $spiro$-OMeTAD and Z1012 decreased by 39.9% and 21.5%, respectively, of their initial values after 4 weeks storing at room temperature under ambient air condition. Previous report showed that when $spiro$-OMeTAD was doped with Li-TFSI and TBP, the pinholes form in the film during spin-coating,, which is considered to be the main reason for decomposition of CH$_3$NH$_3$PbI$_3$ layer in the mesoporous structured PSCs [43]. Moreover, Li-TFSI absorbs moisture in the air, which degrades the perovskite [44]. Also TBP can react with the perovskite by forming a [PbI$_2$·tBP] coordinated complex. Alternatively iodine may react with the tBP to form an iodopyridinate complex [45,46]. Thus, the decrease in device performance of the doped $spiro$-OMeTAD is mainly due to the presence of additives. Furthermore, the hydrophobicity of Z1012 and Z1013 layer can protect the perovskite film damaged by the humidity present in atmosphere.

Aging the PSCs at 80 °C for 3 weeks confirmed that the Z1012 and Z1013 based devices present a better stability than that based on $spiro$-OMeTAD (Fig. S3b). The absence of deliquescent doping additives mainly contribute to this improvement [47,48]. The higher Tg of Z1012 and Z1013 than $spiro$-OMeTAD can also contribute to the better stability of the Z1012 and Z1013 base devices [49].

3. Conclusions

In conclusion, We synthesized two star-shaped triphenylamine (TPA) based small-molecule hole-transporting materials Z1012 and Z1013. These two materials presents suitable energy levels, good thermal stability and high hole mobility, indicating that they can be excellent HTMs for CH$_3$NH$_3$PbI$_3$-based perovskite solar cells. In the presence of Z1013 as HTM without dopants, a PCE of 15.4% was achieved, which is comparable to that of devices based on the well-known doped HTM $spiro$-OMeTAD (16.7%). Importantly, these two HTMs based devices presented better stability when aging in ambient air both at room tempreture and 80 °C in the dark.

Acknowledgements

Appendix A. Supplementary data

Supplementary data related to this article can be found at http://dx.doi.org/10.1016/j.dyepig.2016.08.002.

References

[1] Burschka J, Pellet N, Moon S, Humphry R, Gao P, Nazeeruddin MK, et al. Nature 2013;499:316—9.
[2] Zhang F, Wang SR, Li XG, Xiao Y. Curr Nanosci 2016;12:137—56.
[3] Yang WS, Noh JH, Jeon NJ, Kim YC, Ryu S, Seo J, et al. Science 2015;348:1234—7.
[4] Zhou HP, Chen Q, Li G, Luo S, Song TB, Duan HS, et al. Science 2014;345:542—6.
[5] Kojima A, Teshim K, Shirai Y, Miyasaka T. J Am Chem Soc 2009;131:6050—1.
[6] Bi DQ, Tress W, Dar MI, Gao P, Luo JS, Renevier C, et al. Sci Adv 2016;2:e1501170.
[7] Saliba M, Matsui T, Seo J-Y, Domanski K, Correa-Baena J-P, Nazeeruddin MK, et al. Energy Environ Sci 2016;9:1989—97.
[8] Rakstys K, Abate A, Dar MI, Gao P, Jankauskas V, Jacopin G, et al. J Am Chem Soc 2015;137:16172—8.
[9] Yu Z, Sun LC. Adv Energy Mater. 2015;5:1500213.
[10] Guo JJ, Meng XF, Niu J, Yin Y, Han MM, Ma XH, et al. Synth Met 2016;220:462—8.
[11] Franckevicius M, Mishra A, Kreuzer F, Luo JS, Zakeeruddin SM, Gratzel M. Mater. Horiz 2015;2:613—8.
[12] Kazim S, Ramos FJ, Gao P, Nazeeruddin MK, Gratzel M, Ahmad S. Energy Environ Sci 2015;8:2946—53.
[13] Qin P, Paek S, Dar MI, Pellet N, Ko J, Grätzel M, et al. J Am Chem Soc 2014;136:8516—9.
[14] Zhang F, Yi CY, Wei P, Bi XD, Luo JS, Jacopin G, et al. Adv Energy Mater 2016;6:1600401.
[15] Liu XC, Zhu LF, Zhang F, You J, Xiao Y, Li DM, et al. Energy Technol 2016. http://dx.doi.org/10.1002/ente.201600303.
[16] Liu XY, Zhang F, Liu XC, Sun MN, Wang SR, Li DM, et al. J Energy Chem 2016;25:702—8.
[17] Lv ST, Han LY, Xiao JY, Zhu LF, Shi JJ, Wei HY, et al. Chem Commun 2014;50:6931—4.
[18] Zhu LF, Xiao JY, Shi JJ, Wang JJ, Lv ST, Xu YZ, et al. Nano Res 2015;8:1116—27.
[19] Liu YS, Chen Q, Duan HS, PZhou H, Yang Y, Chen HJ, et al. J Mater. Chem A 2015;3:11940—7.
[20] Liu YS, Hong ZR, Chen Q, Chen HJ, Chang WH, Yang Y, et al. Adv Mater 2016;28:440—6.
[21] Gong GF, Zhao N, Ni DB, Chen JY, Shen Y, Wang MK, et al. J Mater. Chem A 2016;4:3661—6.
[22] Wang YK, Yuan ZC, Shi GZ, Li YX, Li Q, Hui F, et al. Adv Funct Mater 2016;26:1375—81.
[23] Huang CY, Fu WF, Li CZ, Zhang ZQ, Qiu WM, Shi MM, et al. J Am Chem Soc 2016;138:2528—31.
[24] Kanibolotsky AL, Perepichka IF, Skabara PJ. Chem Soc Rev 2010;39:2695—728.
[25] Lai WY, Xia R, He QY, Levermore PA, Huang W, Bradley DDC. Adv Mater 2009;21:355—60.
[26] Wong WWH, Singh TB, Vak D, Pisula W, Yan C, Feng X, et al. Adv Funct Mater 2010;20:927—38.
[27] Chen L, Li P, Cheng Y, Xie Z, Wang L, Jing X, et al. Adv Mater 2011;23:2986—90.
[28] Do K, Choi H, Lim K, Jo H, Cho JW, Nazeeruddin MK, et al. Chem Commun 2014;50:10971—4.
[29] Lim K, Kang MS, Myung, J.H. Seo, P. Banerjee, T.J. Marks Y, et al. J Mater Chem A 2016;4:1186—90.
[30] Choi H, Ko HM, Ko J. Dyes Pigments 2016;126:179—85.
[31] Choi H, Park S, Paek S, Ekanayake P, Nazeeruddin MK, Ko J. J Mater Chem A 2014;2:19136—40.
[32] Kang MS, Sung SD, Choi IT, Kim H, Hong M, Kim J, et al. ACS Appl Mater Interfaces 2015;7:22213—7.
[33] Ramos FJ, Rakstys K, Kazim S, Gratzel M, Nazeeruddinc MK, Ahmad S. RSC Adv 2015;5:53426—32.
[34] Choi H, Cho JW, Kang M-S, Ko J. Chem Commun 2015;51:9305—8.
[35] Wei P, Bi XD, Wu Z, Xu Z. Org Let 2005;7:3199—202.
[36] Yang JS, Chiou SY, Liau KL. J Am Chem Soc 2002;124:2518—27.
[37] Lupton JM, Sameul ID, Burn PL, Mukamel S. J Phys Chem B 2002;106:7647—53.
[38] Krishna A, Sabba D, Li H, Yin J, Boix PP, Soci C, et al. Chem Sci 2014;5:2702—9.
[39] Krishnamoorthy T, Kunwu F, Boix PP, Li H, Koh TM, Leong WL, et al. J Mater Chem A 2014;2:6305—9.
[40] Poplavskyy D, Nelson J. J Appl Phys 2002;93:341—6.
[41] Xu B, Sheibani E, Liu P, Zhang JB, Tian HN, Vlachopoulos N, et al. Adv Mater 2014;26:6629—34.
[42] Kim HS, Park NG. J Phys Chem Lett 2014;5:2927—34.
[43] Tiep NH, Ku Z, Fan HJ. Adv Energy Mater 2016;6:1501420.
[44] Berhe TA, Su WN, Chen CH, Pan CJ, Cheng JH, Chen HM, et al. Energy Environ Sci 2016;9:323—56.
[45] Li W, Dong H, Wang L, Li N, Guo X, Li J, et al. J Mater Chem A 2014;2:13587—92.
[46] Greijer H, Lindgren J, Hagfeldt A. J Phys Chem B 2001;105:6314—20.
[47] Zhang FG, Yang XC, Cheng Ming, Wang WH, Sun LC. Nano Energy 2016;20:108—16.
[48] Liu J, Wu YZ, Qin CJ, Yang XD, Yasuda T, Islam A, et al. Energy Environ Sci 2014;7:2963—7.
[49] Malinauskas T, Tomkute-Luksiene D, Sens R, Daskeviciene M, Send R, Wonneberger H, et al. ACS Appl Mater Interfaces 2015;7:11107—16.